Clinical Applicability of Current Pharmacokinetic Models: Splanchnic Elimination of 5-Fluorouracil in Cancer Patients

Peter J. Robinson,[1] Ludvik Bass,[1,5] Susan M. Pond,[2] Michael S. Roberts,[3] and John G. Wagner[4]

What can be inferred from limited clinical data by using current models of hepatic elimination? We examined this question by analyzing previously published data on the steady-state uptake of the anticancer agent 5-fluorouracil (5-FU) in seven cancer patients in terms of the venous equilibration model, the undistributed and distributed forms of the sinusoidal perfusion model, and the convection–dispersion model. Because of appreciable extrasplanchnic removal of 5-FU, the value of the steady infusion rate was not used in our analysis. When the data from all patients were pooled by plotting the measured hepatic venous concentration against the measured hepatic arterial concentration, the high concentration data fell on a limiting straight line of slope 1, indicating that at high dose rates elimination of 5-FU in both the liver and gastrointestinal tract was close to saturation. The intercept of this line gave a model-independent estimate of $V_{max}/Q = 48.0 \pm 11.6$ (SD) μM for the pooled data set, where V_{max} is the maximum splanchnic elimination rate of 5-FU, and Q is the hepatic blood flow. The low concentration data points fell on a limiting straight line through the origin, from which model-dependent values of the Michaelis constant were determined. The venous equilibration model gave $K_m = 9.4 \mu M$, while the undistributed sinusoidal perfusion model gave $K_m^* = 26.5 \mu M$. With these values of K_m, both models fit the pooled data equally well. These methods were applied to analyses of the five individual data sets which contained sufficiently high concentration data points. The resulting mean values were $V_{max}/Q = 41.0 \pm 5.1$ (sem) μM, $K_m = 8.4 \pm 1.3 \mu M$ and $K_m^* = 23.2 \pm 3.2 \mu M$. However, the splanchnic region is a highly heterogeneous organ system, for which an undistributed analysis provides no more than an upper bound on the Michaelis constant K_m^+ ($K_m^+ \leq K_m^*$). A perfusion model distributed to represent total splanchnic elimination is developed in the Appendix. Using

---

[1]Department of Mathematics, University of Queensland, Brisbane, Australia.
[2]Department of Medicine, University of Queensland, Brisbane, Australia.
[3]School of Pharmacy, University of Otago, Dunedin, New Zealand.
[4]College of Pharmacy, Department of Pharmacology and Upjohn Center for Clinical Pharmacology, University of Michigan, Ann Arbor, Michigan.
[5]To whom correspondence should be addressed at Department of Mathematics, University of Queensland, St. Lucia, Queensland 4067, Australia.

previous estimates of the degree of functional heterogeneity in the liver alone, this model yields
K_m^+ *values for individual patients which have a mean of 20.3 ± 2.8 μM.*

KEY WORDS: Michaelis–Menten kinetics; sinusoidal perfusion model; venous equilibration model; distributed model; convection-dispersion model; organ heterogeneity; bioavailability; pooling of data; kinetic parameter estimation.

INTRODUCTION

When substrates of hepatocellular enzymes are eliminated rapidly enough to display a first-pass effect and a hepatic clearance dependent on hepatic blood flow, any quantitative account of elimination and bioavailability of the substrate must somehow be related to hepatic physiology. Several quantitative liver models have been proposed for this purpose, and ingenious experiments with animal livers (both isolated and *in situ*) have been performed in order to discriminate between the models by precise statistical analyses. Such discrimination is not intended here. The present authors have put aside their differing views as to the relative merits of the models in order to examine another question: What is the impact of the several models on a particular set of clinical data from human subjects, typically more limited and less precise than data from animal preparations? Whatever may be the result of future discrimination between the models, interpretations of such data are the ultimate object of the modeling.

5-Fluorouracil (5-FU) has been used extensively for the treatment of solid tumors in man. It is eliminated by the liver, kidney, and other extrahepatic sites (1–3) but not by the lung (4). In particular, 5-FU is eliminated to a significant extent in the gastrointestinal (GI) tract (3). Chadwick and Rogers (2) found substantial concentrations of the metabolite α-fluoro-β-ureidopropionic acid (FUPA) in the epithelium of the GI tract after intravenous injection of 5-FU in mice, indicating that enzymes for metabolic degradation of the drug are located in these epithelial cells.

In a recent study, Wagner *et al.* (5) investigated the hepatic elimination of 5-FU in man by making a series of three to six steady-state intravenous infusions of 2 hr duration in seven cancer patients, while sampling the concentration of 5-FU in the hepatic artery (C_{HA}) and the hepatic vein (C_{HV}). (Abbreviations, symbols, and Units used are shown in Table I.) Figure 1 presents a schematic diagram of the circulation showing the sites of the infusion and sampling catheters. The principal aim of the present paper is to devise methods to analyze this and other similar data sets in order to determine, for each individual patient, the appropriate kinetic parameters for uptake. We develop a method that is as far as possible independent of the assumptions of any particular mathematical model and unaffected by extrasplanchnic elimination. When a specific model of uptake

Table I. Abbreviations, Symbols, and Units

|	
5-FU	5-Fluorouracil
C_{HA}, C_{HV}	Concentrations of 5-FU in hepatic artery and hepatic vein (μM)
$\bar{C}$	Logarithmic mean of C_{HA} and C_{HV} [Eq. (4)] (μM)
Q	Total hepatic blood flow (L min^{-1}, or cm^3 sec^{-1})
λ	Fraction of Q passing through portal vein
V	Elimination rate of 5-FU in splanchnic region (μmole min^{-1})
I	Total steady infusion of 5-FU (μmole min^{-1})
V_{max}	Maximum splanchnic elimination rate of 5-FU (μmole min^{-1})
V_{max}^{L}, V_{max}^{G}	Maximum elimination rate of 5-FU in liver and GI tract, respectively (μmole min^{-1})
K_m	Michaelis constant (μM)
*,†	Superscripts referring to parameters estimated by the undistributed and distributed sinusoidal perfusion model, respectively
F_i	Intrinsic bioavailability
Cl_i	Intrinsic clearance of total drug (L min^{-1})
ε, ε_L, ε_G	Measures of the degree of functional heterogeneity in the total splanchnic region, in the liver alone, and in the GI tract alone
R	A positive remainder term [Eqs. (13) and (15)]
ρ	Hepatocellular enzyme density along sinusoids (cm^{-1})
A	Total cross-sectional area for flow through liver (cm^2)
L	Effective length of liver (cm)
D	Dispersion coefficient for substrate passing through liver (cm^2 sec^{-1})
D_N	Dispersion number
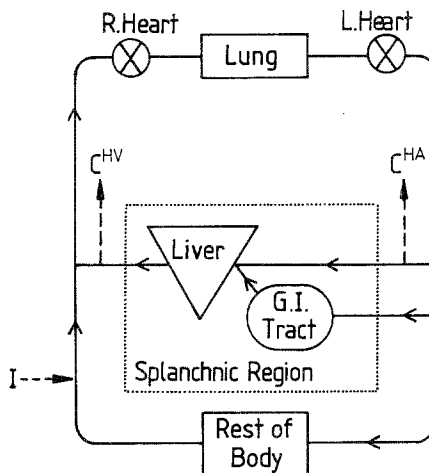
Fig. 1. Schematic diagram of the circulation, showing sites of sampling catheters in the hepatic artery (C_{HA}) and in the hepatic vein (C_{HV}), and the site of peripheral infusion I used in Wagner *et al.* (5). The dotted line encompasses the splanchnic region, consisting of the liver and the GI tract, connected by the portal vein.

is necessary (as in the determination of the Michaelis constant K_m), the data are analyzed according to a number of models currently in use, and their corresponding estimates of parameters are compared.

As elimination is steady, the concentration at entry to the GI tract is the same as C_{HA}. Applying Fick's law in the steady state to the whole splanchnic region gives

$$V = Q(C_{HA} - C_{HV}) \qquad (1)$$

where V is the elimination rate of 5-FU in the splanchnic region consisting of the liver plus the GI tract (Fig. 1), and Q is the total hepatic blood flow. Because no blood samples were taken from the portal vein between the GI tract and the liver, it is not possible to apportion the total splanchnic elimination rate V between the liver and the GI tract. In our analysis of these data we therefore consider splanchnic elimination as a whole.

Because extrasplanchnic elimination of 5-FU in man is considerable (1), the splanchnic elimination rate V in Eq. (1) is less than the total steady-state infusion rate, I. This is supported by the result of Wagner et al. (5) that if V is replaced by I in Eq. (1), then each set of data I, C_{HA}, C_{HV} gives a calculated value of Q much greater than hepatic blood flow (as high as the cardiac output). We therefore calculate V directly from Eq. (1) using measured steady-state values for C_{HA} and C_{HV}, and either measured or estimated values for the hepatic blood flow Q.

In order to estimate kinetic parameters for the splanchnic uptake of 5-FU in man, a model for such elimination in the liver and the GI tract is required. A number of models currently in use describe the saturable uptake of substances by the intact liver. These include the undistributed sinusoidal perfusion model (6); the venous equilibration model (7-9); the distributed sinusoidal perfusion model (10), and the convection-dispersion model (11-13). Although all these models assume that Michaelis-Menten kinetics hold for the interaction of substrate and enzyme, they differ in their assumptions about the manner of presentation of substrate to enzyme in the physiological setting. The *venous equilibration model* assumes that all hepatocytes are presented with the concentration of substrate observed in the emergent venous blood. This model was developed for the liver alone and is inappropriate for elimination by the entire splanchnic region. (Are the enzymes in the GI tract to operate at a substrate concentration equal to that in the hepatic vein?) The *undistributed sinusoidal perfusion model* (6,14) is only slightly more realistic in this case. This model assumes that the entire organ consists of functionally identical passageways (sinusoids), lined with enzymes, through which the substrate passes and is progressively depleted, and that all sinusoids output the same substrate concentration into the hepatic vein. However, considering the typical division of the

hepatic blood flow between the hepatic artery and the portal vein, approximately two-thirds of the substrate passes through both the GI tract and the liver, while the rest passes through the liver alone (Fig. 1). Such heterogeneity in the handling of substrate must be taken into account. This can be accomplished in two related ways. First, the GI tract and the liver can be modeled separately and then put together into a composite model, with the hepatic arterial blood mixing with the portal venous blood from the GI tract to form the input for the liver. A model of this kind is described in the Appendix. More generally, the splanchnic region as a whole can be described in terms of a single distributed (heterogeneous) model. Two such models have been developed and are currently in use to describe hepatic elimination of substrate.

The *distributed sinusoidal perfusion model* (10) allows sinusoidal blood flows and enzyme contents to vary among sinusoids, with substrate output from each sinusoid mixing in the hepatic vein to form the measured output concentration C_{HV}. The output concentration from such a heterogeneous liver is always greater than that from an equivalent undistributed liver with the same input concentration, and with the same total enzyme content and blood flow, divided equally among all sinusoids (10). More recently, the concept of independent, noninteracting sinusoids has been modified to allow for the effects of intrahepatic mixing sites (13). The *convection–dispersion model* of Roberts and Rowlands (11,12) allows heterogeneity of substrate transits through the liver by a different process: it abandons entirely the concept of independent sinusoids in favor of combining unidirectional convection with a generalized term to account for dispersion of substrate passing through the liver.

All four models of hepatic elimination have markedly different mathematical forms and therefore may make quite different predictions as to the outcome of experiments, particularly if these experiments involve changes in hepatic blood flow. Although both the undistributed sinusoidal perfusion model and the venous equilibration model have received some experimental support, both these models have been refuted (11–20). Despite such experimental refutations, and the fact that these two models are inappropriate to describe total splanchnic elimination in detail, they have the advantage of not requiring an additional parameter to specify the heterogeneity in flow and enzyme activity. It is therefore useful to analyze the data of Wagner *et al.* (5) in terms of both these models (as well as the more appropriate distributed models). As all models share certain limiting features, some kinetic parameters, but not others, depend on the choice of model. In particular, the maximum elimination capacity of the liver (plus GI tract) is model-independent, whereas the Michaelis constant K_m is highly model-dependent. The value of K_m obtained by fitting the data to the undistributed

perfusion model has the additional use of providing an upper bound to any K_m obtained by fitting the same data to the distributed perfusion model.

MODELS OF HEPATIC ELIMINATION

The venous equilibration model (7-9) asserts that all hepatocytes are exposed to substrate concentrations equal to the hepatic venous concentration C_{HV}. For Michaelis-Menten kinetics, the elimination capacity of the liver is then given by

$$V = V_{max}\left[\frac{C_{HV}}{C_{HV} + K_m}\right] \qquad (2)$$

where V_{max} is the maximum hepatic elimination rate, and K_m is the Michaelis constant.

The undistributed perfusion model (6), on the other hand, takes into account the depletion of substrate along the hepatic blood flow so that hepatocytes further downstream are exposed to progressively lower substrate concentrations. Those at the arterial end operate at the common input (arterial) substrate concentration C_{HA}, while those at the venous end operate at the concentration C_{HV}. The total elimination rate is then given by (6)

$$V = V_{max}^*\left[\frac{\hat{C}}{\hat{C} + K_m^*}\right] \qquad (3)$$

where

$$\hat{C} = (C_{HA} - C_{HV})/\ln(C_{HA}/C_{HV}) \qquad (4)$$

is the logarithmic mean of C_{HA} and C_{HV}: $C_{HA} > \hat{C} > C_{HV}$. When applied to the same data set of C_{HA}, C_{HV} values, these two models generally yield different values of the kinetic parameters V_{max} and K_m. We thus follow the convention of Wagner et al. (5) and denote values fitted by the sinusoidal perfusion model with asterisks [Eq. (3)] while omitting them from values fitted by the venous equilibration model [Eq. (2)]. The measurable quantities C_{HA}, C_{HV}, and V are common to all models.

Limiting Straight Lines

For high venous substrate concentrations, $C_{HV} \gg K_m$ in Eq. (2); $\hat{C} \gg K_m^*$ in Eq. (3), we have, using also Eq. (1)

$$V = Q(C_{HA} - C_{HV}) = V_{max} = V_{max}^* \qquad (5)$$

Thus, at sufficiently high substrate concentrations, the hepatic elimination rate approaches a maximum value that is common to all models that assume

Michaelis-Menten kinetics locally: all the enzyme molecules are saturated. In a plot of C_{HV} against C_{HA}, we thus expect from Eq. (5) a limiting straight line at high concentrations, with a slope of 1 and an intercept with the abscissa at $C_{HA} = V_{max}/Q = V_{max}^*/Q$. In what follows, we assume that the maximum elimination capacity of the liver can be determined in such a model-independent manner from its elimination rate measured at concentrations close to those for enzyme saturation. We therefore drop the asterisk on V_{max} determined from the sinusoidal perfusion model. Indeed, at high substrate concentrations, Eq. (5) applies to *all* models, including the distributed perfusion and dispersion models: If all enzyme molecules are saturated and working at maximum capacity, the maximum elimination rate of substrate for the organ as a whole is simply the sum total of enzymatic maximum elimination rates, regardless of how those enzymes are distributed among the sinusoids, or the manner of extent of dispersion of substrate within the liver. Thus Eq. (5) represents the limiting straight line for all models at high substrate concentration, yielding a model-independent estimate of V_{max}/Q.

At the opposite extreme of low substrate concentrations, another limiting straight line is found in a plot of C_{HV} vs. C_{HA}. For $C_{HV} \ll K_m$ in Eq. (2) we have, using Eq. (1) and rearranging

$$\frac{C_{HV}}{C_{HA}} = \frac{1}{1 + \dfrac{V_{max}}{QK_m}} \tag{6}$$

On the other hand, for $\hat{C} \ll K_m^*$ in Eq. (3) we have, again using Eq. (1)

$$V = Q(C_{HA} - C_{HV}) = V_{max}\frac{\hat{C}}{K_m^*} \tag{7}$$

Using the definition of $\hat{C}$ [Eq. (4)] and canceling $(C_{HA} - C_{HV})$ from both sides, we obtain, on rearrangement

$$\frac{C_{HV}}{C_{HA}} = e^{-V_{max}/QK_m^*} \tag{8}$$

Equation (8) is derived in a more general way in Bass *et al.* (6), where it is shown that Eq. (8) holds provided either that $V/QK_m^* \ll 1$ or that $V/V_{max} \ll 1$.

Both Eqs. (6) and (8) describe a direct proportionality between C_{HV} and C_{HA} at low substrate concentrations

$$C_{HV} = F_i C_{HA} \tag{9}$$

where the constant of proportionality F_i is the intrinsic bioavailability, defined as the low concentration (first-order) limit of (C_{HV}/C_{HA}). The

interpretation of F_i in terms of the kinetic parameters, particularly K_m, is highly model dependent. For the venous equilibration model we have, from Eqs. (6) and (9)

$$F_i = \frac{1}{1 + \dfrac{V_{max}}{QK_m}} = \frac{1}{1 + \dfrac{Cl_i}{Q}} \tag{10}$$

where $Cl_i = V_{max}/K_m$ is the intrinsic hepatic clearance of total drug according to the venous equilibration model. For the sinusoidal perfusion model, on the other hand, Eqs. (8) and (9) give

$$F_i = e^{-V_{max}/QK_m^*} = e^{-Cl_i^*/Q} \tag{11}$$

where $Cl_i^* = V_{max}/K_m^*$ is the intrinsic clearance according to the undistributed perfusion model. The intrinsic bioavailability F_i is determined directly from the data and is model-independent. It is the interpretation of F_i in terms of the kinetic parameters that is highly model-dependent, with Eqs. (10) and (11) giving interpretations of F_i according to the venous equilibration and sinusoidal perfusion models respectively. We note that Eq. (11) can be written, on expanding the exponential, as

$$F_i = \frac{1}{e^{Cl_i^*/Q}} = \frac{1}{1 + Cl_i^*/Q + \frac{1}{2}(Cl_i^*/Q)^2 + \cdots} \tag{12}$$

It is important to notice that if the development of the denominator is broken off after the linear term and the resulting expression is combined with Fick's law [Eq. (1)], one gets the same relation between F_i and Q as Eq. (10) in the venous equilibration model: hence $Cl_i^* \approx Cl_i$ ($K_m^* \approx K_m$) from any given data. The two models differ therefore inasmuch as the terms so discarded are quantitatively important. It follows that the smaller Cl_i^*/Q, the less the predictions of the two models differ (11). The distributed sinusoidal perfusion model and the convection–dispersion model also predict limiting straight lines in a plot of C_{HV} against C_{HA} at both high and low substrate concentrations.

In the first-order limit of low substrate concentrations the distributed sinusoidal perfusion model predicts the following relation between C_{HA} and C_{HV} (15)

$$F_i = \frac{C_{HV}}{C_{HA}} = \exp\left\{ -\frac{V_{max}}{QK_m^+} + \frac{1}{2}\varepsilon^2 \left[\frac{V_{max}}{QK_m^+}\right]^2 - R \right\} \tag{13}$$

where ε is the coefficient of variation of the (flow-weighted) distribution of maximum sinusoidal arterial-venous concentration differences, and is a measure of the degree of functional heterogeneity of the liver. For a liver

made up of a number of sinusoidal groups in parallel ("notional sub-organs"), each consisting of identical sinusoids and having its own $V_{max}^{(p)}$ and $Q^{(p)}$, where $\Sigma_p \, V_{max}^{(p)} = V_{max}$ and $\Sigma_p Q^{(p)} = Q$, it has been shown that ε^2 is given by (19)

$$\varepsilon^2 = \sum_p \frac{(V_{max}^{(p)}/V_{max})^2}{Q^{(p)}/Q} - 1 \tag{14}$$

The superscript "p" is chosen to denote parallel elements. R is a positive remainder term for which there are precise upper and lower bounds, provided that ε is small enough for the quantity $v_0 = 1/\varepsilon - \varepsilon V_{max}/QK_m^*$ to be positive (15):

$$-\ln\left\{ 1 - \frac{e^{-v_0^2/2}}{\sqrt{2\pi}\left[\dfrac{v_0}{2} + \dfrac{v_0^2}{4} + 1\right]} \right\} < R \leq -\ln\left\{ 1 - \frac{e^{-v_0^2/2}}{\sqrt{2\pi}\left[\dfrac{v_0}{2} + \dfrac{v_0^2}{4} + \dfrac{2}{\pi}\right]} \right\} \tag{15}$$

It is apparent that as ε^2 decreases, R falls off much faster than ε^2.

The symbol $(+)$ is placed on the K_m in Eq. (13) to indicate that the K_m fitted to data according to the distributed model in general differs from K_m^* fitted by the undistributed model and K_m fitted by the venous equilibration model. For experimentally determined values of F_i, V_{max}, and Q, it follows from a comparison of Eqs. (8) [or (11)] and (13) that $K_m^+ \leq K_m^*$ [provided that $R \ll \frac{1}{2}\varepsilon^2(V_{max}/QK_m^+)^2$]. Thus the distributed sinusoidal perfusion model fits the same low concentration-limiting straight line in a plot of C_{HV} against C_{HA} by assigning a smaller value to K_m^+ than K_m^*. In general, the larger the degree of heterogeneity (represented by the parameter ε), the more K_m^+ falls below K_m^*. Thus K_m^* provides a useful upper bound on K_m^+ in cases where the magnitude of ε cannot be estimated directly.

The recently introduced convection–dispersion model of Roberts and Rowland (11,12) adds a generalized dispersion term (acting in the direction of flow) to the convection of substrate through the liver. In the limit of first-order uptake of substrate, there is a mathematical correspondence between the dispersion coefficient D so introduced (mathematically analogous to, though much greater than, the molecular diffusion coefficient of the substrate) and the coefficient of variation ε of the distributed model (11,13)

$$\varepsilon^2 = 2\frac{\overline{\rho^2}}{\bar{\rho}^2}\frac{AD}{QL} \tag{16}$$

where A is the total cross-sectional area for flow through the liver, and ρ is the hepatocellular enzyme density along the effective length L of the liver; $\bar{\rho}$ and $\overline{\rho^2}$ are the mean and mean-square values of ρ, and the ratio $\overline{\rho^2}/\bar{\rho}^2 \geq 1$ expresses the effect of nonuniformity of enzyme distributions in

the direction of flow (13). The dimensionless quantity AD/QL, called the dispersion number D_N, must be $\ll 1$ for the relation (16) to hold. In the first-order limit, therefore, the convection–dispersion model also predicts a straight line through the origin in a plot of C_{HV} against C_{HA}, with the slope F_i given by Eq. (13) (with $R=0$), and ε of the distributed sinusoidal perfusion model identified with the corresponding quantity in the convection-dispersion model, given by Eq. (16).

ANALYSIS OF DATA

Pooled Data

We now turn in detail to the data of Wagner et al. (5), in which the steady-state hepatic arterial and hepatic venous concentrations of 5-FU were measured during steady infusions of 5-FU into a peripheral vein (Fig. 1). From three to six infusions were performed on each of seven patients. Figure 2 shows these data in the form of a plot of C_{HV} against C_{HA}. Such straightforward pooling of data of this form is successful because
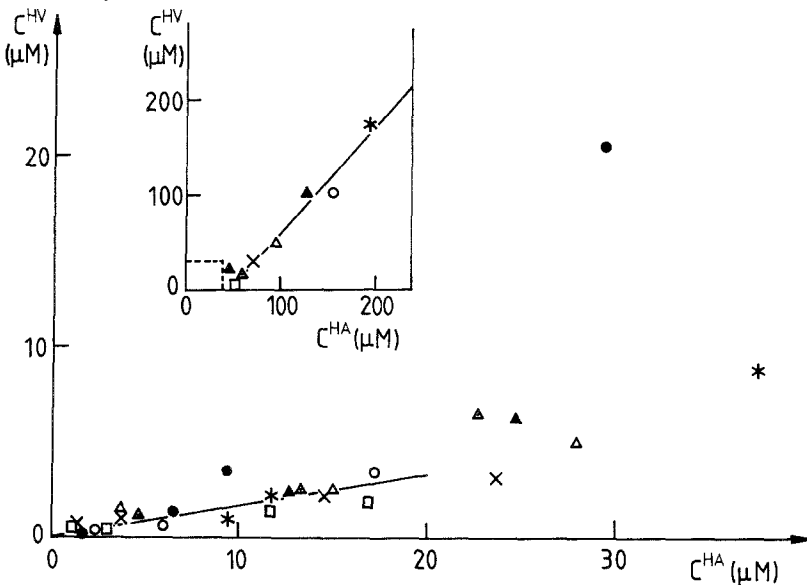

Fig. 2. Plot of steady-state hepatic venous concentration C_{HV} vs. hepatic arterial concentration C_{HA} in seven cancer patients. Data are from Wagner et al. (5). The straight line is the linear regression through 20 data points with $C_{HA} < 20\mu$M, constrained to pass though the origin. Inset shows high concentration data points ($C_{HA} > 40\mu$M). The straight line represents the linear regression through the five highest concentration points, which intercepts the abscissa at $V_{max}/Q = 48.0 \pm 11.6$ (SD) μM and has a slope of 1.09 ± 0.14 (SD).

at both high and low substrate concentrations the limiting straight lines are determined in all models by the ratio V_{max}/Q (as well as by K_m) and not by V_{max} and Q separately: see Eqs. (5), (6), (8), and (13). Thus biological variations in liver mass, to which both V_{max} and Q would be expected to be roughly proportional, cancel at both these limits. Such pooling would not in general be as successful at intermediate substrate concentrations where V_{max} and Q exert their influences separately.

The limiting straight lines described in the section "Models of Hepatic Elimination" are recognizable in Fig. 2. Independent estimates of K_m for uptake of 5-fluorouracil by isolated rat hepatocytes (21) are between 12 and 37 μM. Consistent with these values, examination of Fig. 2. indicates that data points with $C_{HA} \gtrsim 70 \, \mu$M may be considered as determining the high concentration-limiting straight line, Eq. (5). A linear regression through these five highest concentration points has a slope of 1.09 ± 0.14 (SD) and an intercept $V_{max}/Q = 48.0 \pm 11.6$ (SD) μM (see Fig. 2, inset). The slope is not significantly different from unity, which implies that at such high concentrations of 5-FU, elimination by both the liver and the GI tract is saturated. This precludes the possibility of significant elimination of 5-FU in the GI tract by a nonsaturable process such as passive loss into the intestinal lumen. This is consistent with the results of Chadwick and Rogers (2), who showed that after intravenous injections of 5-FU, metabolites of 5-FU found in the gastrointestinal endothelium and in the liver were similar. This indicates that similar enzymatic elimination processes are taking place in the GI tract as in the liver.

The limiting straight line through the origin is apparent for data points with $C_{HA} \lesssim 20 \, \mu$M, $C_{HV} \lesssim 5 \, \mu$M ($\hat{C} \lesssim 10 \, \mu$M). This range is consistent with K_m values measured for isolated rat hepatocytes (21). We thus use the 20 lowest concentration data points to estimate F_i using Eq. (9) by means of linear regression constrained to pass through the origin (Fig. 1), giving $F_i = 0.163$. This intrinsic bioavailability, F_i, given directly by observables, is model-independent. However, its interpretation in terms of the kinetic parameters K_m, V_{max}, and Q is model-dependent. For the venous equilibration model, F_i is given by Eq. (10). Using $V_{max}/Q = 48.0 \, \mu$M gives $K_m = 9.4 \, \mu$M, while for the same value of V_{max}/Q the sinusoidal perfusion model [Eq. (11)] gives $K_m^* = 26.5 \, \mu$M. Without an estimate of the degree of functional heterogeneity of the total splanchnic region consisting of liver plus GI tract, characterized by the parameter ε^2, we cannot make an outright estimate of K_m^+, the value of the Michaelis constant predicted by Eq. (13) of the distributed sinusoidal perfusion model. However, as noted in "Models of Hepatic Elimination," $K_m^+ \leq K_m^*$, so that $K_m^+ \leq 26.5 \, \mu$M from the pooled data of Wagner et al. (5). Closer estimates of K_m^+ are given in the Appendix and Conclusions.

We note that in the context of the venous equilibration model, the 20 data points used to determine F_i have C_{HV} values less than about 40% of our estimated value of K_m (9.4 μM), thus validating their use in the determination of F_i. The five highest concentration data points have C_{HV} values more than three times the estimated value of K_m, justifying their inclusion in the determination of V_{max}/Q. Similarly for the sinusoidal perfusion model, the highest value of $\hat{C}$ of the 20 data points used in the determination of F_i is less than one-third of K_m^* (26.5 μM), whereas the 5 highest concentration data points have $\hat{C}$ values of more than 1.8 times K_m^*.

Analysis of Individual Patients

Using the information gained from our analysis of the pooled data from all seven cancer patients studied by Wagner et al. (5) (by their Method 1), we devised methods for analyzing the fewer data from each individual patient. In particular, only four of the seven individual data sets included a steady-state hepatic arterial concentration $C_{HA} \geq 70\ \mu$M. (This included Patient #4, who was studied on two separate occasions). From our study of the pooled data (Fig. 2), we saw that the slope of the straight line through the five highest concentration data points was not statistically significantly different from 1, indicating saturation of both the liver and the GI tract at these concentrations. We therefore calculated V_{max}/Q for each of these patients from their single highest concentration data point using Eq. (5). (This is equivalent, in a plot of C_{HV} against C_{HA}, to drawing a straight line with slope 1 through the relevant point, with the intercept of this straight line with the abscissa giving V_{max}/Q.) Values of V_{max}/Q calculated in this way are given in Table II, and have a mean value of 41.0 ± 5.1 (SEM) μM, compared with 48.0 μM for the pooled data.

The intrinsic bioavailability F_i can be determined for each individual patient in the same way as for the pooled data set, by forming a linear regression through the lowest concentration data points C_{HV}, C_{HA}, constrained to pass through the origin. Restricting ourselves to values of $C_{HA} \leq 20\ \mu$M as before, we find that most patients have three or more data points in this range (Table II). Values of F_i calculated for individual patients are given in Table II. The mean of the individual F_i determinations is 0.179 ± 0.023 (SEM), which compares with $F_i = 0.163$ obtained from the pooled data.

As with the pooled data analysis, in order to determine K_m values from the individual F_i values, a particular liver model must be chosen. For the venous equilibration model, Eq. (10) was used with individual values of V_{max}/Q (where available) to determine the K_m values given in Table II. These have a mean of 8.4 ± 1.3 (SEM) μM. For the sinusoidal perfusion

Table II. Summary of Parameter Estimates from Individual Patients

Patient	$V_{max}/Q^{(a)}$ (μM)	F_i	$Q^{(c)}$ (L min^{-1})	V_{max} (μmole min^{-1})	$V_{max}/QK_m{}^d$	V_{max}/QK_m^{*d}	V_{max}/QK_m^{+e}	K_m (μM)	K_m^* (μM)	K_m^+ (μM)
1	56.5	0.178(3)^b	—	—	4.62	1.73	1.97	12.2	32.7	28.7
2	42.8	0.147(3)	—	—	5.80	1.92	2.18	7.4	22.7	19.6
3	—	0.107(4)	—	—	8.35	2.24	2.69	—	—	—
4	42.8	0.191(2)	0.490	21.0	4.24	1.66	1.88	10.1	25.9	22.8
4'	48.7	0.174(2)	0.490	23.9	4.75	1.75	2.00	10.2	27.7	24.4
5	28.5	0.174(1)	0.978	27.9	4.75	1.75	2.00	6.0	16.3	14.3
6	—	0.317(3)	0.500	—	2.16	1.15	1.25	—	—	—
7	26.9	0.143(2)	—	—	5.94	1.94	2.27	4.5	13.9	11.9
Mean	41.0	0.179			5.08	1.77	2.03	8.4	23.2	20.3
± SEM	5.1	0.023			0.66	0.12	0.15	1.3	3.2	2.8

^{a} Obtained from single point, $C_{HA} \geq 70 \mu$M, where available.
^{b} Number in parentheses indicates points $\leq 20 \mu$M available for linear regression through origin.
^{c} Hepatic blood flow was measured only in patients 4 (4'), 5, 6.
^{d} V_{max}/QK_m and V_{max}/QK_m^* were obtained from F_i using Eqs. (10) and (11) for the venous equilibration and sinusoidal perfusion models, respectively.
^{e} V_{max}/QK_m^+ was calculated for the distributed sinusoidal perfusion model from Eq. (13), with $R = 0$ and $\epsilon^2 = 0.125$.

model, we used Eq. (11), again with individual V_{max}/Q values to obtain K_m^* values with a mean of 23.2 ± 3.2 (SEM) μM. These compare favorably with values obtained from the pooled data of 9.4 μM and 26.5 μM for the venous equilibration and sinusoidal perfusion models respectively.

Values for the hepatic blood flow Q were measured directly in three patients (Table II), allowing values of the maximum elimination rate V_{max} to be determined from the V_{max}/Q ratios. These values ranged from 21.0 to 27.9 μmole min^{-1} (Table II).

CONCLUSIONS

When C_{HA} and C_{HV} are measured across the Michaelis-Menten range of concentrations (above and below K_m), two model-independent quantities may be determined, one from the limit of high (saturating) substrate concentrations, and the other from the first-order limit at low substrate concentrations, at which C_{HV} is proportional to C_{HA}. At high concentrations, a plot of C_{HV} against C_{HA} for all seven patients studied by Method 1 of Wagner et al. (5) tends to a limiting straight line with a slope not significantly different from 1 (Fig. 2, inset), indicating that elimination in both the liver and GI tract is saturated. This result precludes significant first-order elimination in the GI tract (for example, by diffusion of 5-FU into the lumen). The intercept of the limiting straight line with the abscissa gives an estimate of V_{max}/Q for the pooled data, where $V_{max} = V_{max}^L + V_{max}^G$ is the sum of the maximum elimination rates of the liver and the GI tract, of 48.0 ± 11.6 (SD) μM (see the section "Analysis of Data" and Fig. 2, inset). The contributions of the liver and the GI tract to this total could not be separated because the 5-FU concentration in the portal vein was not sampled. Estimates of V_{max}/Q for individual patients are given in Table II. In those cases in which a value for the hepatic blood flow Q is also available, an estimate of V_{max} is also given in Table II. Estimates of V_{max}/Q (or V_{max}) calculated in this way are common to all the models of elimination discussed in this paper, and are thus considered model-independent in the present context.

At the other extreme of low substrate concentrations ($C_{HA} \ll K_m$), all models predict direct proportionality between C_{HV} and C_{HA}: a plot of C_{HV} against C_{HA} tends towards a limiting straight line through the origin as low substrate concentrations are approached. Such a limiting straight line is clearly observed in Fig. 2 in the pooled 5-FU uptake data of Wagner et al. (5). However, the models differ markedly in their interpretation of the slope of this straight line—the intrinsic bioavailability F_i—in terms of the parameters V_{max}, Q, and K_m. Thus, for the pooled data, the venous equilibration model gives an estimate of K_m of 9.4 μM, whereas the undistributed sinusoidal perfusion model gives $K_m^* = 26.5$ μM. With these values of K_m,

both models fit the data equally well (for the totality of pooled data points, the sum of squares of differences between predicted and measured values of C_{HV} are 1338 and 1505 μM^2 for the venous equilibration and sinusoidal perfusion models, respectively). It is interesting (though not essential in our analysis) that both these values of K_m are close to or within the range of between 12 μM and 37 μM reported for isolated rat hepatocytes by Mentre *et al.* (21).

As noted in the Introduction, the anatomy and the arrangement of blood flow through the total splanchnic region do not lend themselves to a direct application of either the venous equilibration or the undistributed sinusoidal perfusion model, even if we disregard the refutations of these models in isolated livers (11–13, 15–18, 20). In addition, analyses of the uptake of various substrates by the intact liver have shown that the liver alone has a significant degree of functional heterogeneity characterized by the parameter ε^2 (see, for example, refs. 10, 15, 19, 20). In the Appendix we therefore outline a composite model of the splanchnic region in which a minimum degree of heterogeneity is taken into account. The liver and GI tract are modeled according to the distributed and undistributed forms of the sinusoidal perfusion model, respectively. A composite eliminating organ is then modeled by assuming that blood from the hepatic artery mixes with blood from the portal vein before entry into the liver. The heterogeneity of this model is characterized by the parameter ε given by Eq. (A3). Gustavsson *et al.* (3) have estimated that in mice, some 15% of total 5-FU elimination occurs in the GI tract, while about 23% is eliminated in the liver (at an infusion rate of 5-FU of 0.625 mg kg^{-1} hr^{-1}). Assuming that these ratios roughly reflect the relative magnitudes of V_{max}^G and V_{max}^L (in humans), then Eq. (A3) becomes:

$$\varepsilon^2 = 0.39\left(\frac{1}{\lambda} - 1\right) + 0.61\varepsilon_L^2 \tag{17}$$

where λ is the fraction of the total hepatic blood flow Q that passes through the portal vein (see Appendix).

Past estimates of ε_L^2 for the liver alone include $\varepsilon_L^2 = 0.12$ for the uptake of taurocholate by isolated perfused rat livers [data of Pries *et al.* (22), analyzed in ref. 13]; $\varepsilon_L^2 = 0.137$ for uptake of colloidal $CrPO_4$ by rat liver [data of Bauer *et al*, (14), analyzed in ref. 15]; $\varepsilon_L^2 \leq 0.182$ for galactose uptake by rat liver [data of Keiding and Chiarantini (17), analyzed in ref. 23], and $\varepsilon_L^2 = 0.196$ for galactose elimination by isolated pig livers [data of Keiding *et al.* (24), analyzed in ref. 20]. No estimates of ε_L^2 for normal human livers exist in the literature. However, it has been shown for galactose elimination that in one cirrhotic patient (data from K. Winkler, private communication), about 36% of total hepatic blood flow is shunted past the

functional enzymes (25). Such intrahepatic shunts are a special case of heterogeneity, and an equivalent value for ε_L^2 corresponding to a particular shunt can be calculated (19); for a 36% shunt, $\varepsilon_L^2 = 0.56$. It is, however, unlikely that normal human livers would have such a high degree of intrahepatic shunting.

The magnitude of K_m^+ estimated by means of the distributed sinusoidal perfusion model depends on ε^2 according to Eq. (13): the larger ε^2, the smaller is the estimated value of K_m^+. The size of ε^2 in turn depends on ε_L^2 according to Eq. (17). For the pooled 5-FU uptake data of Wagner *et al.* (5), $F_i = 0.163$ and $V_{max}/Q = 48.0\ \mu M$; for $R = 0$, the calculated values of K_m^+ as a function of ε_L^2 are shown in Fig. 3 for $\lambda = 0.7$, 0.75 and 0.8. Also shown in Fig. 3 are calculated values of K_m and K_m^* from the venous equilibration and undistributed sinusoidal perfusion models (horizontal arrows). Values of ε_L^2 previously estimated from other data sets are shown as vertical arrows on the abscissa. For $\varepsilon_L^2 = 0.20$ and $\lambda = 0.75$ we have from Fig. 3 that $K_m^+ = 23\ \mu M$, and from Eq. (17) that $\varepsilon^2 = 0.125$. From Eq. (15) the remainder term R lies in the range $0.018 < R \le 0.019$, which is less than 10% of the previous term in the expansion (13), thus justifying its neglect in our calculations of K_m^+ in this case. For larger values of ε_L^2, R becomes relatively larger: for $\varepsilon_L^2 = 0.56$, R is more than one-third of the previous term in Eq. (13). At such high values of ε_L^2, estimates of K_m^+ given by Fig. 3 can be used only as a rough guide. Values of K_m^+ calculated according to Eq. (13) with $R = 0$, $\varepsilon^2 = 0.125$ and using values of V_{max}/Q for individual patients, are given in Table II. They have a mean value of 20.3 ± 2.8 (SEM) μM, which is within 13% of the upper bound to K_m given by the undistributed sinusoidal perfusion model.

The foregoing numerical estimates of kinetic parameters show that the several models differ substantially in their interpretations of the data, so that an ultimate decision between the models is desirable. It is also apparent that such a decision cannot be reached on the basis of clinical data alone: Modeling theory is at present ahead of experiment in the sense that clinical data do not determine all the model parameters unambiguously. We do not view this as a deficiency of the models, because one of the roles of theory is to motivate future experimental designs and methods of measurement.

Whereas validation of models is best based on studies of groups of subjects, the ultimate use of the models pertains to individual patients, as attempted here. Estimates of the kinetic parameters V_{max} and K_m have evident clinical importance for individual patients, especially for the choice of dosage of toxic drugs such as 5-FU. Whereas a steady infusion rate $I < V_{max}$ results in a steady, controlled concentration in the body, an increase of I to a value exceeding V_{max} leads to concentrations tending to arbitrarily large values. While an estimate of V_{max} is thus especially useful for choices
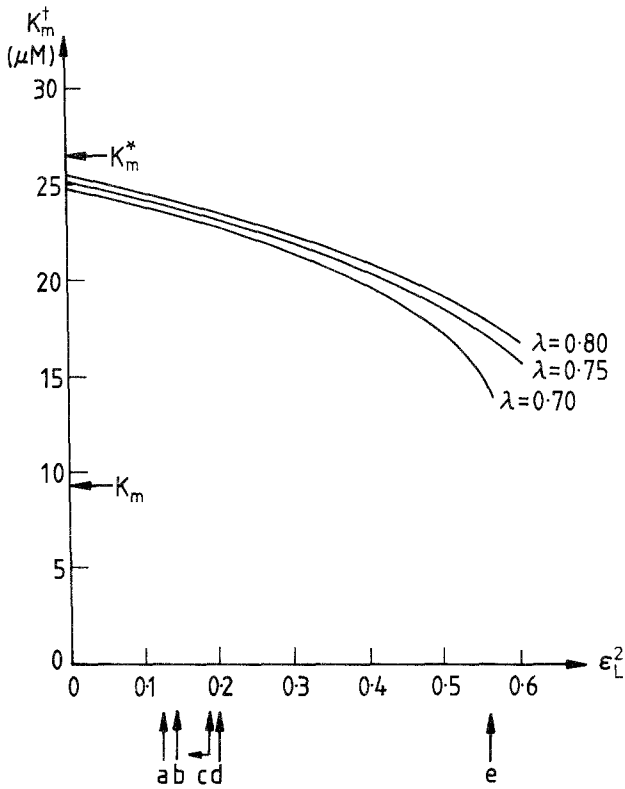
Fig. 3. Variation of K_m^+ with the degree of heterogeneity ε_L^2 of the liver, from the pooled data of Wagner *et al.* (5) and based on the distributed sinusoidal perfusion model [Eq. (13)], with $V_{max}/Q = 48.0\ \mu M$, $F_i = 0.163$ and $R = 0$. Curves are drawn for three values of the fraction (λ) of the total hepatic blood flow passing through the portal vein. Total splanchnic heterogeneity ε is given by Eq. (17). Note that for $\varepsilon_L^2 = 0$, K_m^+ is still slightly less than K_m^* estimated from the undistributed model (upper horizontal arrow) due to heterogeneity associated with the GI tract-hepatic artery system. The lower horizontal arrow shows K_m estimated by the venous equilibration model. Vertical arrows on the abscissa show previously estimated values of ε_L^2: (a) taurocholate elimination by isolated rat livers (13,22); (b) colloidal $CrPO_4$ elimination by RE system of rat liver (14,15); (c) and (d) galactose elimination by isolated pig livers (17, 20, 23, 24); (e) galactose elimination by cirrhotic human liver (25).

of steady infusions, an estimate of K_m for each individual patient is useful for controlling the delivery of drugs in bolus inputs. As long as the substrate concentration in the bolus is well below K_m (first-order kinetics), the hepatic extraction fraction is independent of concentration and hence of dose delivery. When the bolus concentration approaches and exceeds K_m, the extraction fraction falls as concentration is increased: in the limit $V \to V_{max}$, the hepatic extraction fraction tends to zero, and bioavailability C_{HV}/C_{HA} tends to unity. As the onset of these nonlinear phenomena is controlled by the value of K_m, its estimate (together with that of V_{max}) for each individual patient is a prerequisite of rational dosing. Furthermore, changes in the hepatic extraction fraction with changes in hepatic blood flow (in exercise, cardiac failure, after meals, etc.) and with pathological changes in liver heterogeneity (as in intrahepatic shunting in cirrhosis) are of clinical interest. These considerations illustrate the clinical importance of the choices and uses of the models of hepatic elimination.

APPENDIX: ELIMINATION BY LIVER PLUS GI TRACT

We describe a composite model for steady-state Michaelis-Menten elimination of a substrate by both the liver and the GI tract, as shown schematically in Fig. 4. Blood with substrate at a concentration C_{HA} enters both the hepatic artery and the GI tract at flow rates $(1-\lambda)F$ and λF respectively, where F is the rate of total hepatic blood flow and λ is the fraction of F that is contributed by the portal circulation (Figs. 4 and 1).

Substrate is eliminated from the blood during passage through the GI tract, which outputs into the portal vein. We adopt the common assumption of complete prehepatic mixing of portal and hepatic arterial blood. As a
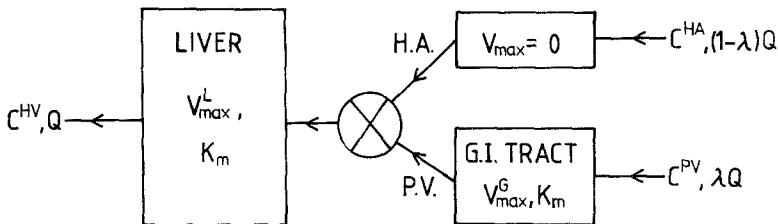

Fig. 4. Schematic diagram of composite model of splanchnic region described in the Appendix, consisting of three suborgans. Arterial blood, concentration C_{HA}, enters the hepatic artery and the portal circulation passing through the GI tract, with flows of $(1-\lambda)Q$ and λQ respectively, where Q is total hepatic blood flow. Substrate is eliminated in the GI tract but not in the hepatic artery; blood from these two parallel suborgans is then mixed before entering the liver, where substrate is further eliminated before being output into the hepatic vein at a concentration C_{HV}.

result of hepatic elimination, the observed hepatic venous concentration is C_{HV}.

Let the maximum elimination capacity of the liver be given by V_{max}^L, and that of the GI tract by V_{max}^G. Let us assume that the elimination process is such that the Michaelis constant K_m is the same in both liver and GI tract. This assumption is consistent with the finding of similar metabolites of 5-FU in the epithelium of the GI tract as in the liver following intravenous injections of 5-FU in mice (2). The splanchnic region as a whole can then be represented schematically as in Fig. 4, consisting of three suborgans. Of these, the GI tract and the hepatic artery are functionally in parallel (the hepatic artery acts essentially as a shunt). In series with these is the liver itself which receives as its input the mixed output from the GI tract and the hepatic artery. Let us assume, for simplicity, and in the absence of any data concerning its functional heterogeneity, that the GI tract eliminates substrate according to the undistributed sinusoidal perfusion model. Then the composite organ, representing the GI tract and hepatic artery in parallel, can be characterized by the parameter ε_G which can be calculated from Eq. (14). Letting $Q^{(1)} = \lambda Q$, $V_{max}^{(1)} = V_{max}^G$ for the GI tract, and $Q^{(2)} = (1 - \lambda) Q$, $V_{max}^{(2)} = 0$ for the hepatic artery shunt gives, from Eq. (14)

$$\varepsilon_G^2 = \frac{1}{\lambda} - 1 \qquad (A1)$$

Since we have neglected any contributions to heterogeneity from the GI tract alone, Eq. (A1) represents a lower bound to the true ε_G^2.

The splanchnic region is now reduced to two suborgans in series: the GI tract/hepatic artery suborgan, with ε_G^2 given by Eq. (A1), and the liver itself, with heterogeneity characterized by ε_L^2. These two suborgans are connected by an intraorgan mixing site. The method of calculation of the composite value for ε^2 for a number of distributed suborgans in series, each separated by a site of mixing, has been described previously for first-order uptake of substrate (13), and is given by

$$\varepsilon^2 = \sum_s \varepsilon_{(s)}^2 \left[\frac{V_{max}^{(s)}}{V_{max}} \right]^2 \qquad (A2)$$

where s denotes elements in series, and where V_{max} is the total maximum elimination capacity. In our present example, $\varepsilon_{(1)}^2 = \varepsilon_G^2$, $V_{max}^{(1)} = V_{max}^G$, and $\varepsilon_{(2)}^2 = \varepsilon_L^2$, $V_{max}^{(2)} = V_{max}^L$, so that Eq. (A2) gives for the splanchnic region as a whole

$$\varepsilon^2 = \left(\frac{1}{\lambda} - 1 \right) \left[\frac{V_{max}^G}{V_{max}} \right]^2 + \varepsilon_L^2 \left[\frac{V_{max}^L}{V_{max}} \right]^2 \qquad (A3)$$

where $V_{max} = V_{max}^{G} + V_{max}^{L}$. Equation (17) is an application of this result. Thus, in the first-order limit, the composite model of the splanchnic region shown in Fig. 4 is described in terms of a single distributed sinusoidal perfusion model with a maximum elimination rate $V_{max} = V_{max}^{G} + V_{max}^{L}$, and the value for ε^2 given by Eq. (A3).

REFERENCES

1. J. L. Speyer, P. H. Sugarbaker, J. M. Collins, R. L. Dedrick, R. W. Klecker, Jr., and C. E. Myers. Portal levels and hepatic clearance of 5-fluorouracil after intraperitoneal administration in humans. *Cancer Res.* **41:**1916–1922 (1981).
2. M. Chadwick and J. Rogers. The physiological disposition of 5-fluorouracil in mice bearing solid L1210 lymphocytic leukemia. *Cancer Res.* **32:**1045–1056 (1972).
3. B. G. Gustavsson, A. Brandberg, C. G. Regardh, and O. E. Almersjo. Regional and systemic serum concentration of 5-fluorouracil after portal and intravenous infusion: an experimental study in dogs. *J. Pharmacokin. Biopharm.* **7:**665–673 (1979).
4. Y.-H. Kao, C.-Y. Yang, R. R. L. Chen, and J.-D. Huang. Pulmonary elimination of 5-fluorouracil in anesthetized rats. *J. Pharm. Sci.* **74:**1095–1096 (1985).
5. J. G. Wagner, J. W. Gyves, P. L. Stetson, S. C. Walker-Andrews, I. S. Wollner, M. K. Cochran, and W. P. Ensminger. Steady-state nonlinear pharmacokinetics of 5-fluorouracil during hepatic arterial and intravenous infusions in cancer patients. *Cancer Res.* **46:**1499–1506 (1986).
6. L. Bass, S. Keiding, K. Winkler, and N. Tygstrup. Enzymatic elimination of substrates flowing through the intact liver. *J. Theor. Biol.* **61:**393–409 (1976).
7. J. R. Gillette. Factors affecting drug metabolism. *Ann. N.Y. Acad. Sci.* **179:**43–66 (1971).
8. M. Rowland, L. Z. Benet, and G. G. Graham. Clearance concepts in pharmacokinetics. *J. Pharmacokin. Biopharm.* **20:**123–136 (1973).
9. R. A. Branch, A. S. Nies, and D. G. Shand. The disposition of propranolol VIII. General implications of the effects of liver blood flow on elimination from the perfused rat liver. *Drug Metab. Dispos.* **1:**687–690 (1973).
10. L. Bass, P. J. Robinson, and A. J. Bracken. Hepatic elimination of flowing substrates: The distributed model. *J. Theor. Biol.* **72:**161–184 (1978).
11. M. S. Roberts and M. Rowland. Hepatic elimination—dispersion model. *J. Pharm. Sci.* **74:**585–587 (1985).
12. M. S. Roberts and M. Rowland. A dispersion model of hepatic elimination. *J. Pharmacokin. Biopharm.* **14:**227–308 (1986).
13. L. Bass, M. S. Roberts, and P. J. Robinson. On the relation between extended forms of the sinusoidal perfusion and of the convection-dispersion models of hepatic elimination. *J. Theor. Biol.* **126:**457–482 (1987).
14. R. W. Brauer, G. F. Leong, R. F. McElroy, and R. J. Holloway. Circulatory pathways in the rat liver as revealed by P^{32} chromic phosphate colloid uptake in the isolated perfused liver preparation. *Am. J. Physiol.* **184:**593–598 (1956).
15. L. Bass. Flow-dependence of first-order uptake of substances by heterogeneous perfused organs. *J. Theor. Biol.* **86:**365–376 (1980).
16. K. S. Pang and M. Rowland. Hepatic clearance of drugs. II. Experimental evidences for acceptance of the "well stirred" model over the "parallel tube" model using lidocaine in the perfused rat liver *in situ* preparation. *J. Pharmacokin. Biopharm.* **5:**655–680 (1977).
17. S. Keiding and E. Chiarantini. Effect of sinusoidal perfusion on galactose elimination kinetics in perfused rat liver. *J. Pharmacol. Exp. Ther.* **205:**465–470 (1978).
18. S. Keiding and E. Steiness. Flow dependence of propranolol elimination in perfused rat liver. *J. Pharmacol. Exp. Ther.* **230:**474–477 (1984).
19. L. Bass. Saturation kinetics in hepatic drug removal: a statistical approach to functional heterogeneity. *Am. J. Physiol.* **244:**G583–G589 (1983).

20. L. Bass and P. J. Robinson. Effects of capillary heterogeneity on rates of steady uptake of substances by the intact liver. *Microvasc. Res.* **22:**43–57 (1981).
21. F. Mentre, J. L. Steimer, J. P. Sommadossi, R. B. Diasio, and J. P. Cano. A mathematical model of the kinetics of 5-fluorouracil and its catabolites in freshly isolated rat hepatocytes. *Biochem. Pharmacol.* **33:**2727–2732 (1984).
22. J. M. Pries, A. B. Staples, and R. F. Hanson. Effect of hepatic blood flow on taurocholate extraction by the isolated perfused rat liver. *J. Lab. Clin. Med.* **97:**412–417 (1981).
23. L. Bass and P. J. Robinson. How small is the functional variability of liver sinusoids? *J. Theor. Biol.* **81:**761–769 (1979).
24. S. Keiding, S. Johansen, K. Winkler, K. Tonnesen, and N. Tygstrup. Michaelis–Menten kinetics of galactose elimination by the isolated pig liver. *Am. J. Physiol.* **230:**1302–1313 (1976).
25. P. J. Robinson. Aspects of mathematical liver kinetics: the steady-state statistical mechanics of hepatic elimination. Ph.D. thesis, University of Queensland. (University Microfilms International, Ann Arbor, Michigan, 1979)